

Reversibly erasable nanoporous anti-reflection coatings from polyelectrolyte multilayers

JERI'ANN HILLER, JONAS D. MENDELSON AND MICHAEL F. RUBNER*

Department of Materials Science and Engineering, Massachusetts Institute of Technology, Cambridge, Massachusetts 02139, USA

*e-mail: rubner@MIT.edu

Published online: 2 September 2002; doi:10.1038/nmat719

For nearly two centuries, researchers have sought novel methods to increase light transmission in optical systems, as well as to eliminate unwanted reflections and glare. Anti-reflection coatings and surfaces have enabled the increasing performance demands of optical components fabricated from glass-based optical materials. With the current trend of technology moving towards optically transparent polymeric media and coatings, the need for anti-reflection technology and environmentally benign processing methods for polymeric materials independent of shape or size has become quite apparent. We describe an economical, aqueous-based process controlled at the molecular level that simultaneously coats all surfaces of almost any material. Systematically designed nanoporous polymer films are used, which are suitable for optical applications operating at both visible and near-infrared wavelengths. These high-efficiency anti-reflection coatings are created from phase-separated polyelectrolyte multilayer films that undergo a reversible pH-induced swelling transition. Furthermore, such films, easily patterned by an inkjet printing technique, possess potential for pH-responsive biomaterial and membrane applications.

Anti-reflection coatings play a pivotal role in a wide variety of optical technologies by reducing reflective losses at interfaces. Optical elements based on glass and common plastics have indices of refraction (n) in the range of 1.45–1.7 (refs 1,2) and, as a result, reflect from 4% to more than 6.5% of normal incident light from each air–substrate interface. The additive energy loss of reflected radiation can be especially detrimental to a system's performance when there are several optical components involved. In applications such as flat-panel displays for electronics, anti-reflection coatings are employed to eliminate the effects of 'ghost images', or veil glares originating from stray and multiple reflections from optical surfaces. Reflection losses from optical components are notably disadvantageous in technologies such as solar-cell collectors, which rely on efficiently transmitted energy. It is therefore necessary to reduce the intensity of reflected light to improve the overall quality, performance and efficiencies of such systems, which translates to increasing transmission, improving contrast and reducing glare, as well as eliminating ghost images.

A reduction in surface reflection is typically accomplished by the application of an anti-reflection coating of a quarter-wavelength optical thickness. When the index of refraction of the coating (n_c) is equivalent to the square root of the product of the indices of the surrounding medium (n_o) and the substrate (n_s), that is, $n_c = (n_o n_s)^{0.5}$, reflections are suppressed at wavelengths near the quarter-wavelength optical thickness¹. Consequently, n must be between 1.2 and 1.3 for efficient anti-reflection coatings to be suitable for glass and polymeric optical elements. This is, in general, a difficult task because readily available low n materials are limited to values of ~ 1.35 (ref. 1). One solution to this problem is to use appropriately designed porous materials, that is, materials possessing homogeneously distributed pores much smaller than the wavelength of light, such that light scattering from the pores is limited as described above. Such materials can possess a very low effective n , due to the introduction of air³, which has an n of 1. To achieve broadband anti-reflection properties, it is further necessary to create a graded n , such that n_c close to the substrate surface matches n_s and decreases to lower values further away from the surface^{1,4}. Surfaces possessing a gradient in n over sufficient depth, such as the cornea of the moth's eye, show minimized reflection over a broad range of wavelengths and angles of incidence⁵.

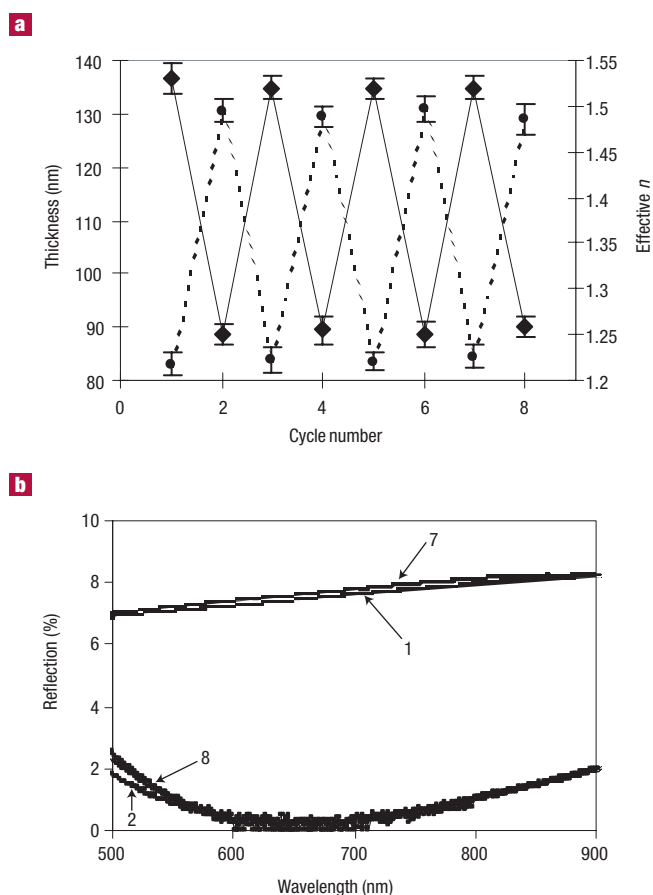


Figure 1 pH-switchable optical properties of PAH/PAA multilayer films.

a, Thickness (dashed line) and effective n measured by ellipsometry at 633 nm (solid line) as a function of the 'cycle number' for a 7.5-bilayer PAH/PAA film assembled on silicon; cycling occurs between a porous and non-porous state. Data for cycles 1, 3, 5 and 7 were obtained after the film was immersed into water at pH 1.8 for 60 s and subsequently dried with compressed air. The data for cycles 2, 4, 6 and 8 were obtained after a 15 s pH 5.5 aqueous rinse of the sample subjected to cycles 1, 3, 5 and 7, respectively. **b**, Near-normal reflection versus wavelength of a PAH/PAA multilayer film, prepared in a similar manner as the film in **a**, coated on both sides of a polystyrene substrate. 1, 2, 7 and 8 refer to the cycle numbers shown in **a**.

Not surprisingly, porous surfaces and materials have been extensively explored for anti-reflection applications. Early approaches with glass used phase-separation and etching processes to create porous surfaces^{4,6}. More recent approaches include sol-gel processes⁷ and the adsorption of colloids onto polyelectrolyte multilayers⁸, among others. Nanoporous polymer coatings created by the selective dissolution of spin-coated films have also recently been explored^{9,10}. Although such coatings show efficient anti-reflection properties, they are not well suited for the application of a uniform, defect-free coating to large areas, highly contoured or textured substrates, or, for example, the inner surfaces of tubes. In addition, these coating applications require the use of solvents, which pose environmental hazards and could potentially swell or dissolve certain polymeric substrates. Hence, despite the fact that low n nanoporous materials are ideal candidates for anti-reflection coatings, there are numerous challenges associated with processing them into optical-quality, conformal coatings for large areas that would be suitable for many different types of optical elements.

In this work, we show that aqueous-processed polyelectrolyte multilayers assembled one molecular layer at a time by an electrostatically

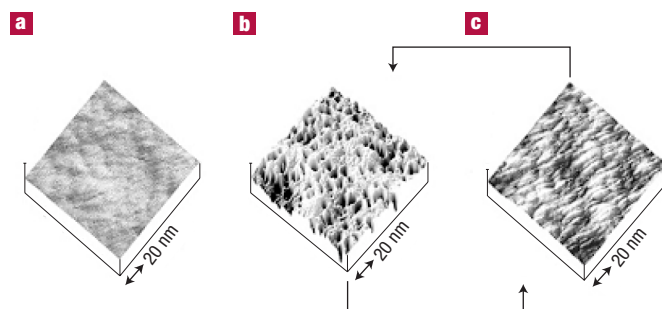


Figure 2 Reversible nanoporosity in PAH/PAA. $1 \times 1 \mu\text{m}^2$ AFM three-dimensional images of the multilayer film on silicon substrates. **a**, The original non-porous structure. **b**, The nanoporous structure with apparent pore depths of ~ 60 nm. **c**, The non-porous structure created during pH cycling. The z-range of the images shown is 100 nm.

driven process^{11–13} can be transformed into nanoporous thin films with an effective n that can be controllably tuned from ~ 1.5 to 1.15. We also demonstrate that thin films graded in n are readily possible with this approach, making these films suitable for use as broadband anti-reflection coatings. This versatile process is particularly amenable to the creation of large-area uniform coatings on essentially any surface with precise control over thickness¹⁴ and optical properties. For example, glass, and even more significantly, polymeric surfaces, can be coated to exhibit reflective losses as low as 0.01%, compared with 4–5% per surface for an uncoated substrate. In addition, under specific conditions, the transformation to the nanoporous structure can be completely reversed, making it possible to create reversibly erasable nanoporous thin films. Simple patterning techniques such as inkjet printing^{15–17} can be further exploited to create patterned nanoporous thin films on the micrometre scale, accomplished again through the use of aqueous solutions.

We, and subsequently others, have previously reported that porous thin films can be created from multilayer films of poly(allylamine hydrochloride)/poly(acrylic acid) (PAH/PAA) by a simple aqueous treatment^{18,19}. Specifically, a pH-induced ionic bond-breaking and reformation mechanism in the PAH/PAA system was shown to enable a large-scale morphological reorganization, resulting in microporosity¹⁸. However, the resultant microporous films created in this manner possess pores with diameters in the range of 50–500 nm, thereby rendering them unsuitable for use as anti-reflection coatings owing to their strong propensity to scatter light. We have now discovered that the lengthscale of the porous features created by this process can be advantageously controlled by varying the pH of the porosity-inducing steps, as well as by the addition of low concentrations of various salts, such as NaCl and MgCl_2 , to the acidic bath. As a result, it is now possible to create nanoporous thin films that are ideally suited for anti-reflection applications and, if desired, may be cycled between a porous and non-porous state.

To create a nanoporous film, we first assemble a PAH/PAA multilayer at pH conditions of 8.5 and 3.5 for PAH and PAA, respectively (denoted as 8.5/3.5 PAH/PAA). By immersing the 8.5/3.5 PAH/PAA multilayer into an acidic solution of pH 1.8, a pH-induced phase separation (most probably a spinodal-type), similar to that observed in the microporous PAH/PAA films¹⁸, occurs, due to protonation of the carboxylic acid groups. A brief rinse (~ 15 s) in water at pH 5.5 and subsequent drying results in a swollen, phase-separated, nanoporous multilayer exhibiting a composite n between that of air and that of the polymer film. Re-immersion into the acidic solution results in re-protonation of the carboxylate groups and collapse of the film to a non-porous state. To preserve the reversibility of this process, it was found that the immersion times in the aqueous solutions should not exceed ~ 5 min. It appears that a densification (possibly a coarsening of the spinodal structure) similar to previous

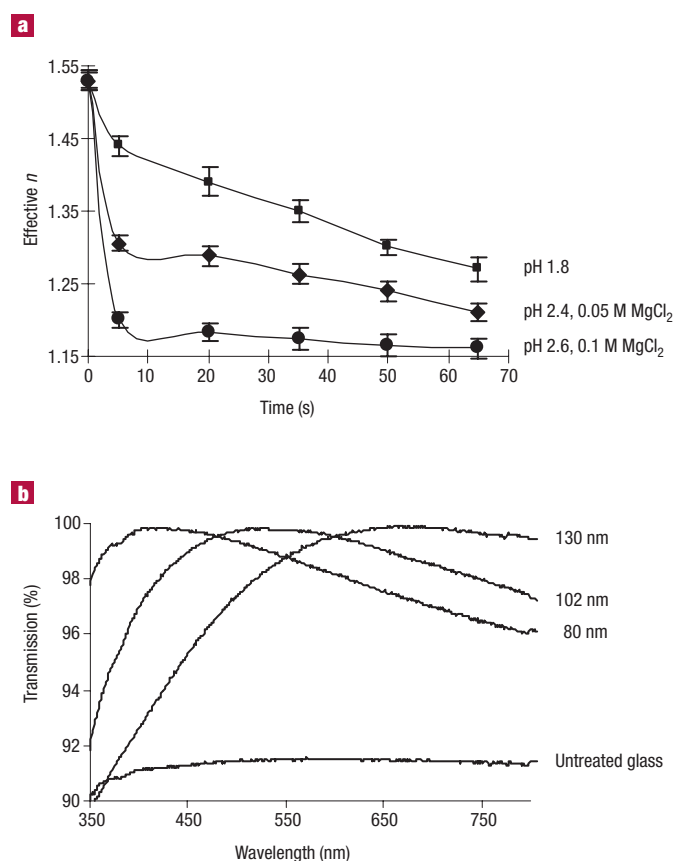


Figure 3 Tuning the optical properties of nanoporous PAH/PAA multilayer films.

a, Evolution of the effective n with time for a 7.5-bilayer PAH/PAA film ~ 90 nm thick. All films were rinsed in pH 5.5 H_2O after the indicated treatment. **b**, Transmission versus wavelength characteristics of glass slides coated with nanoporous films designed to have an effective n of 1.26, and thickness of: 80 nm (5.5 bilayers, 120 s in pH 1.8 aqueous solution, 15-s pH 5.5 aqueous rinse); 102 nm (6.5 bilayers, 75 s in pH 2.3, 0.01 M $MgCl_2$, 15-s pH 5.5 aqueous rinse); and 130 nm (7.5 bilayers, 45 s in pH 2.4, 0.05 M $MgCl_2$, 15-s pH 5.5 aqueous rinse). For comparison the transmission spectrum of untreated glass is also shown.

observations¹⁸, occurs on extended exposure to the aqueous solutions. The effective n of the film described above cycled reproducibly between values of 1.52 and 1.25 as it was reversibly converted from a non-porous to nanoporous state, respectively (Fig. 1a).

The thickness of the phase-separated film alternates from about 85 nm to about 130 nm as a result of the reversible swelling transition. Reflectivity data of a polystyrene substrate coated on both sides with this nanoporous film show that the coating effectively suppresses reflective losses near the quarter-wavelength optical thickness (650 nm) to as low as 0.01% (Fig. 1b). In the non-porous state, the thin film no longer behaves as an anti-reflection coating, and reflective losses, mostly of the polystyrene substrate, are observed (about 7.5%). Atomic force microscopy (AFM) images of the multilayer film (Fig. 2) reveal the nanopores that are reversibly formed during this cycling process; nanoporous features with an apparent depth of ~ 60 nm are only observed when the film is behaving as an anti-reflection coating (Fig. 2b).

In the process described above, the first acidic treatment leads to an irreversible spinodal-like phase-separation¹⁸. The resultant molecular organization is now capable of undergoing a reversible, pH-gated nanoporosity transition. This effective opening and closing of pores is driven by changes in the degree of ionization of the carboxylic acid groups of PAA¹⁸, and the concomitant change in degree of electrostatic repulsion.

Similar phenomena have been used to engineer ‘smart surfaces’ such as pH-responsive polyelectrolytes grafted onto porous membranes²⁰. A similar pH-dependent gating mechanism occurs naturally in the carboxyl cages of the cowpea chlorotic mottle virus²¹. The resultant pH-triggered pore opening and closing facilitates molecular exchange between the virus and its environment^{21,22}. We are currently working to confirm the mechanistic details of the reversible nanoporosity transition in PAH/PAA.

It should be noted that, if desired, the nanoporous multilayer films can be stabilized against further pH-induced morphological transitions by a simple heat-induced crosslinking reaction^{18,23}. This crosslinking step slightly modifies the optical thickness of the film, while imparting improved mechanical robustness to these highly porous structures. The effective n of the nanoporous PAH/PAA multilayer films can be tuned systematically between 1.55 and 1.15 (Fig. 3a). The processing conditions are among those that were experimentally determined to produce optically transparent nanoporous films (as verified by optical-transmission measurements). In general, nanoporous structures suitable for use as anti-reflection coatings are created when the acidic solution in this process is in the pH range of 1.8–1.9. This low-pH range enables sufficient protonation of carboxylic acid groups, which in turn drives the molecular reorganization. Furthermore, the addition of salts such as $MgCl_2$, in concentrations between 0.01 and 0.1 M, means that the pH values must increase to 2.2–2.6 to be able activate this mechanism.

The effective n created by any of these various treatments can be ‘locked-in’ by the crosslinking reaction. AFM imaging indicates that average pore diameter increases in size, to 15–80 nm, as the effective n is lowered. With appropriate processing parameters, highly transparent nanoporous films can be precisely tailored to deliver specific optical as well as physical properties such as surface roughness, wettability and chemical functionality. Although values of n as low as 1.15 have been achieved, the exploration of the wide range of parameter space means that effective indices of refraction of less than 1.1 are expected.

The precise control over film thickness provided by the layer-by-layer processing approach further allows systematic design of the optical properties. For example, adjustments in the processing variables, and the number of deposited PAH/PAA layers on glass slides coated with films of increasing physical thickness, enables the resultant optical thickness of the nanoporous films to be systematically tuned. Therefore coatings that exhibit transmission maxima wherever desired in the visible region of the spectrum are possible (Fig. 3b). The layer-by-layer adsorption process also facilitates the simultaneous application of a conformal anti-reflection coating to all surfaces of an optical substrate, including substrates that are highly contoured and/or substrates with internal surfaces. A photographic image of a polystyrene Petri dish, partially treated with a nanoporous anti-reflection coating and placed on top of printed text, clearly demonstrates the increased transparency and reduced glare of the coated side (Fig. 4a). All surfaces exposed to the aqueous dipping solutions during the multilayer assembly process, including the edges of the Petri dish, are conformally coated with the anti-reflective multilayer thin film. Optical-grade polymers such as polystyrene, polycarbonate and polyacrylics, which normally transmit only about 89% of incident visible light, can exhibit transmission levels $>98\%$ in the visible region when coated with these films. Because plastics possess high tailorability and combine novel physical and mechanical properties, they are ideal candidates for optical components such as photographic and vision-correction lenses.

Another advantage of the processing strategy described here is the potential to create patterned nanoporous PAH/PAA multilayer thin films (Fig. 4b). In this case, the anti-reflective properties of the nanoporous coating make it possible to clearly visualize the pattern. Micrometre-scale patterned thin films of PAH/PAA can be created using a suitably modified commercial inkjet printer^{16,17}. The multilayer film can be ‘printed’ in one of two ways¹⁸: (a) directly with the acidic aqueous solution used to induce porosity, such that patterned regions of

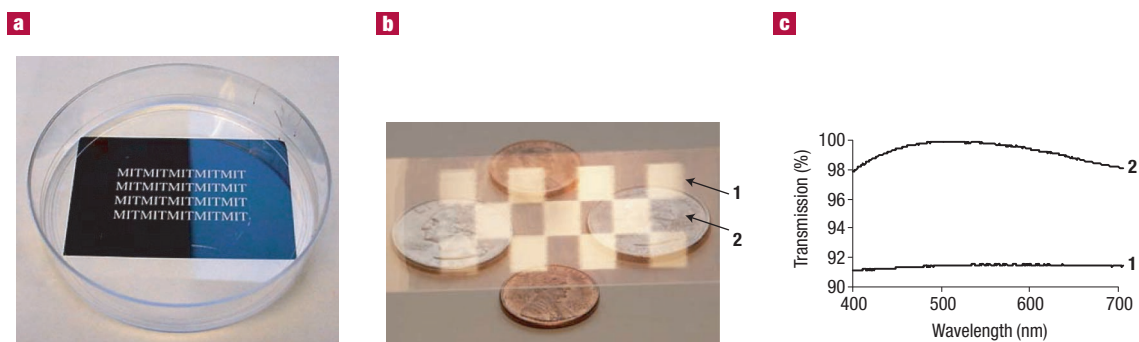


Figure 4 Optical properties of micropatterned, nanoporous PAH/PAA anti-reflection coatings. **a**, Photograph of a polystyrene Petri dish conformally coated on the left half with a 6.5 bilayer PAH/PAA film (assembled at PAH pH 7.75 and PAA pH 3.5) made nanoporous by a 60-s immersion in pH 2.3, 0.01 M MgCl₂ solution, followed by a 15-s, pH 5.5 water rinse. **b**, Photograph of a glass slide with a selectively patterned nanoporous coating composed of 6.5 bilayers of PAH/PAA 7.75/3.5. (assembled at PAH pH 7.75 and PAA pH 3.5). The multilayer film in specified region **1** was dissolved away in pH 1.2 solution using an inkjet printer, whereas the remaining film (**2**) was subjected to a nanoporosity treatment to render it highly transparent. **c**, Wavelength-dependent transmission characteristics of the (**1**) non-porous regions of the glass slide and of the (**2**) anti-reflective regions, as shown in **b**.

nanoporous material are created within the multilayer film; or (b) with an aqueous solution of low enough pH to dissolve the printed regions, in which case the regions not printed (and hence not removed from the substrate) are rendered nanoporous after patterning. Patterns with a resolution of $\sim 50 \mu\text{m}$ can be achieved in this manner. The photographic image (Fig. 4b) shows a glass slide coated with an inkjet-patterned nanoporous film on both sides that was created by using method (b) above. The nanoporous regions of this patterned film exhibit the optical characteristics shown (Fig. 4c). The average transmission of the glass slide is increased from around 91.5% for untreated surfaces to an average of 99%, in the range of 400–700 nm, with a maximum of 99.99% at 520 nm. It should be noted that standard to high efficiency anti-reflection coatings used industrially result in transmission levels that range from 95

to 99% in the visible range. The ability to create micropatterned nanoporous films, which have low dielectric constants and good insulating properties, similar to their microporous counterparts¹⁸, have the potential to be useful in microelectronics applications.

The relatively broadband anti-reflective properties exemplified by the data shown in Fig. 4c suggest that the nanoporous films created by this process have a partially graded index of refraction. This idea is further supported by AFM images (such as Fig. 2b), which show a progressive narrowing of the pore radius with increasing depth towards the substrate and apparent pore penetration depths of ~ 50 – 80 nm (depending on film thickness and processing parameters). However, we recognize that this may be an artefact of the convolution of the AFM tip. To confirm the existence of such a gradation in n , we modelled this apparent gradient as a series of homogeneous layers of progressively higher n (from top to bottom of the film) to generate theoretical transmission and reflection curves by using the matrix theory^{4,24}.

The good agreement between the experimental and theoretical data (Fig. 5) supports the notion that the nanoporous films have a partially graded index of refraction consistent with the AFM images. A similar type of nanocorrugated structure was observed in anti-reflection coatings fabricated from solvent-processed polymer films and, in conjunction with optical data, was presented as evidence for a graded index¹⁰.

To produce an even broader wavelength range of anti-reflection behaviour (and reduced angle dependence), the layer-by-layer process can be used to create multiple (PAH/PAA)-layered blocks of varying n . The latter can be achieved by assembling a set number of PAH/PAA bilayers onto the surface, treating them as described to produce a specific n and then thermally crosslinking the layers to stabilize n against further pH treatments. In this context, a bilayer refers to the combination of a polycation and a polyanion. Additional bilayers of (PAH/PAA) can then be assembled in the same manner to produce the desired gradient.

Using this approach, it is possible to design broadband anti-reflection coatings based entirely on only two polymers (for example, PAH and PAA) that cover any desired wavelength range in the visible to near-infrared spectrum. The measured and calculated transmission curves for a 'double-layered block' design are shown in Fig. 6. Triple-layered-block designs with transmission of more than 98% in the range of 0.4 – $2.5 \mu\text{m}$ have also been demonstrated. It should be noted that the designs discussed are not fully optimized for optical performance, but rather the assembly conditions were chosen to minimize the scattering that can sometimes be introduced by the growth and processing of a (PAH/PAA) block assembled onto a porous (PAH/PAA) film. We fully expect that appropriate assembly conditions can be identified that would allow for full optical optimization over a wide range of wavelengths.

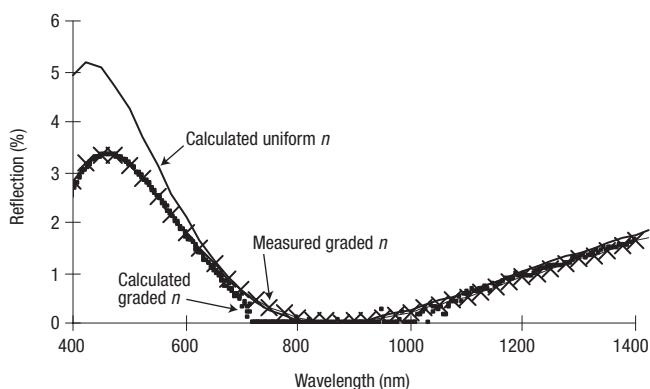


Figure 5 Evidence for the graded n of nanoporous PAH/PAA anti-reflection coatings. Comparison of the calculated and measured near-normal single-surface reflection from a polystyrene substrate coated with 8.5 bilayers of PAH/PAA-rendered nanoporous film by immersion in pH 2.3, 0.03 M MgCl₂ for 45 s and rinsed in neutral water. The measured reflection is well approximated by a linear gradient (a sequence of 20 discrete layers) comprising the top 84 nm of the film varying in n from 1.05 to 1.2 (top to bottom), above a 134-nm-thick layer with an effective n of 1.26. The 84 nm of varying n correspond to the apparent depth of the porous surface features observed by AFM imaging of this nanoporous film on silicon. For comparison, the calculated wavelength-dependent reflection curve of a coating with uniform n of 1.26 and a thickness of 170 nm is also presented.

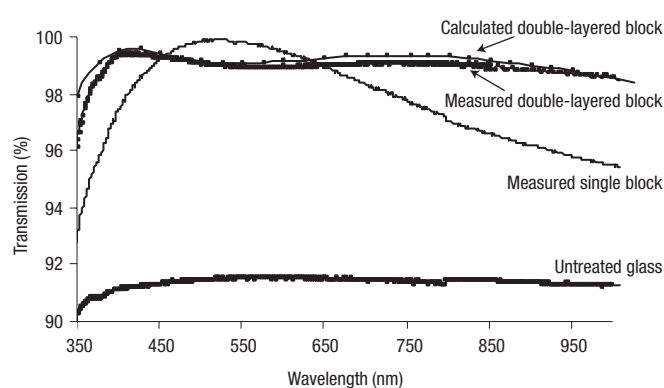


Figure 6A 'double-layered block' design: demonstration of a general design approach. Comparison of the calculated and measured wavelength-dependent transmission curves of a double-layered block structure with a 107-nm-thick top PAH/PAA block (closest to air) having an effective n of 1.225, and a 98-nm-thick bottom PAH/PAA block with an effective n of 1.41. For comparison, also shown are the measured transmission spectrum of a 95-nm-thick single PAH/PAA block with an effective n of 1.26, and the transmission spectrum of untreated glass.

In addition to appropriate optical specifications, useful anti-reflection coatings should also exhibit good mechanical properties such as abrasion resistance, durability and adhesion to substrate materials. Our preliminary findings suggest that the porous films prepared on appropriately surface-modified substrates such as corona-treated plastics (for example the polystyrene used in this study) or silane-treated glass, exhibit excellent adhesion as indicated by a simple adhesive-tape test (in which the tape was firmly applied then peeled briskly from the surface). In addition, such films can withstand gentle buffing with a soft cloth (verified visually and by ultraviolet-visible transmission measurements). We have also found that the addition of inorganic components to the film allows further improvement to their resistance to vigorous buffing with a soft cloth. For example, titania nanoparticle/(PAH/PAA) multilayer composites can be rendered nanoporous and subsequently crosslinked to achieve anti-reflection coatings with n tunable over the range of 1.7–1.2. Further quantitative testing needs to be done to substantiate these assessments.

Although these tunable films of controllable and reversible nanoporosity are ideal for optical technologies such as the anti-reflection coatings demonstrated here, applications including membranes with tunable porosity, and environmentally and pH-responsive controlled-release and drug-delivery systems are similarly promising technologies. This new approach to creating nanoporous films provides an environmentally friendly route to designing versatile, broadband anti-reflection coatings for polymeric and glass surfaces. Although cheap, this entirely aqueous-based process creates coatings engineered at the molecular level that give high-performance, high-transmission, anti-reflection and anti-glare properties to surfaces of substrates of any size, shape or material. Defect- and pinhole-free transparent coatings are therefore created, having optical properties that can be readily tuned.

METHODS

SOURCES OF MATERIALS

PAH ($M_w \approx 70,000$) (Aldrich) and PAA ($M_w \approx 90,000$, 25% aqueous solution) (Polysciences) were used as received and prepared as 10^{-2} M solutions (based on the repeat-unit molecular weight) in ultrapure 18 M Ω -cm Millipore water. The pH of the PAH and PAA solutions were adjusted, typically to 7.75 or 8.5 for PAH and to 3.5 for PAA. PAH/PAA multilayer thin films were assembled at room temperature, as described previously^{14,18}, on to glass slides, polished <100> silicon wafers, and tissue-culture polystyrene (TCPS) substrates using an HMS programmable slide stainer (Zeiss).

FILM ASSEMBLY

In a typical film assembly, 6.5–10.5 bilayers of PAH/PAA were prepared, with the outermost layer being PAH. After the initial multilayer fabrication, the films were exposed to acidic water, pH-adjusted with 1 M

HCl, with or without additional MgCl₂ of various ionic strengths, usually for 15–120 s and then immediately dried with compressed, filtered air or rinsed briefly (~15 s) in deionized water at pH 5.5 and then dried. Thermal crosslinking was performed as previously described¹⁸. Titania nanoparticle/(PAH/PAA) multilayer composites were prepared by incorporating titania nanoparticles (Nanophase Technologies) into the PAH solution which was adjusted in the pH range of 8.5–10 and subsequently assembled with PAA at a pH of 3.5–7.5.

FILM CHARACTERIZATION

AFM characterization (Digital Instruments Dimension 3000 Scanning Probe Microscope) was performed in tapping mode with Si cantilevers. Average pore diameters were obtained by averaging characteristic sections of the raw AFM data of at least of ten samples processed at a given condition. Film thickness and effective index of refraction were obtained in the usual manner^{14,18} on a Gaertner ellipsometer, operating at 633 nm. Physical thickness values were confirmed by profilometry.

TRANSMISSION AND REFLECTIVITY MEASUREMENTS

Transmission and reflectivity data were acquired on a Cary 500i ultraviolet/visible/near-infrared spectrophotometer. Data were obtained from films assembled on glass or polystyrene substrates. For reflectivity measurements (near-normal) from one side of a substrate, the film was removed from a single side of the substrate, which was then covered with black tape. These data were modelled using matrix theory^{4,23} to evaluate the optical properties of the coatings as well as to corroborate thickness and index of refraction data acquired from ellipsometry and profilometry measurements. A modified inkjet printer^{16,17} was used to pattern nanoporous films. Aqueous solution at pH 1.2 was printed in the desired pattern onto the multilayer film. The film was then immediately rinsed in water at pH 5.5 and dried with compressed, filtered air.

Received 30 June 2002; accepted 6 August 2002; published 2 September 2002.

References

- Macleod, H. A. *Thin-Film Optical Filters* (Elsevier, New York, 1969).
- Mark, J. E. (ed.) *Polymer Data Handbook* (Oxford Univ. Press, New York, 1999).
- Yoldas, B. E. Investigations of porous oxides as an antireflective coating for glass surfaces. *Appl. Opt.* **19**, 1425–1429 (1980).
- Minot, M. J. Single-layer, gradient refractive index antireflection films effective from 0.35 to 2.5 microns. *J. Opt. Soc. Am.* **66**, 515–519 (1976).
- Clapham, P. B. & Hutley, M. C. Reduction of lens reflexion by the 'Moth Eye' principle. *Nature* **244**, 281–282 (1973).
- Fraunhofer, J. *Versuche über die Ursachen des Anlaufens und Mattwerdens des Glases und die Mittel, denselben zu vermeiden* 33–49 (Joseph von Fraunhofer's Gesammelte Schriften, Munich, 1888).
- Uhlmann, D. R., Suratwala, T., Davidson, K., Boulton, J. M. & Teowee, G. Sol-gel derived coatings on glass. *J. Non-Cryst. Solids* **218**, 113–122 (1997).
- Hattori, H. Anti-reflection surface with particle coating deposited by electrostatic attraction. *Adv. Mater.* **13**, 51–54 (2001).
- Walheim, S., Schäffer, E., Mlynek, J. & Steiner, U. Nanophase-separated polymer films as high-performance antireflection coatings. *Science* **283**, 520–522 (1999).
- Ibn-Elhaj, M. & Schadt, M. Optical polymer thin films with isotropic and anisotropic nano-corrugated surface topologies. *Nature* **410**, 796–799 (2001).
- Decher, G., Hong, J. D. & Schmitt, J. Buildup of ultrathin multilayer films by a self-assembly process III. Consecutively alternating adsorption of anionic and cationic polyelectrolytes on charged surfaces. *Thin Solid Films* **210**, 831–835 (1992).
- Decher, G. Fuzzy nanoassemblies: toward layered polymeric multicomposites. *Science* **277**, 1232 (1997).
- Ferreira, M., Cheung, J. H. & Rubner, M. F. Molecular self-assembly of conjugated polyions – a new process for fabricating multilayer thin-film heterostructures. *Thin Solid Films* **244**, 806–809 (1994).
- Shiratori, S. S. & Rubner, M. F. pH-Dependent thickness behavior of sequentially adsorbed layers of weak polyelectrolytes. *Macromolecules* **33**, 4213–4219 (2000).
- Calvert, P. Inkjet printing for materials and devices. *Chem. Mater.* **13**, 3299–3305 (2001).
- Wang, T. C., Chen, B., Rubner, M. F. & Cohen, R. E. Selective electroless nickel plating on polyelectrolyte multilayer platforms. *Langmuir* **17**, 6610–6615 (2001).
- Yang, S. Y. & Rubner, M. F. Micropatterning of polymer thin films with pH-sensitive and cross-linkable hydrogen-bonded polyelectrolyte multilayers. *J. Am. Chem. Soc.* **124**, 2100–2101 (2002).
- Mendelsohn, J. D. et al. Fabrication of microporous thin films from polyelectrolyte multilayers. *Langmuir* **16**, 5017–5023 (2000).
- Fery, A., Scholer, B., Cassagneau, T. & Caruso, F. Nanoporous thin films formed by salt-induced structural changes in multilayers of poly(acrylic acid) and poly(allylamine). *Langmuir* **17**, 3779–3783 (2001).
- Zhang, H. & Ito, Y. in *Handbook of Polyelectrolytes and Their Applications* Vol. I (eds Tripathy, S. K., Kumar, J. & Nalwa, S. S.) 183–197 (American Scientific, California, 2002).
- Speir, J. A., Munshi, S., Wang, G. J., Baker, T. S. & Johnson, J. E. Structures of the native and swollen forms of cowpea chlorotic mottle virus determined by X-ray crystallography and cryo-electron microscopy. *Structure* **3**, 63–78 (1995).
- Douglas, T. & Young, M. Host-guest encapsulation of materials by assembled virus protein cages. *Nature* **393**, 6681–6685 (1998).
- Harris, J. J., DeRose, P. M. & Bruening, M. L. Synthesis of passivating, nylon-like coatings through cross-linking of ultrathin polyelectrolyte films. *J. Am. Chem. Soc.* **121**, 1978–1979 (1999).
- Monaco, S. F. Reflectance of an inhomogeneous thin film. *J. Opt. Soc. Am.* **51**, 280–282 (1961).

Acknowledgements

We thank J.-F. Hiller for computational support. This research was supported financially by the MIT Center for Materials Science and Engineering and the National Science Foundation. J.H. acknowledges the Lucent Technologies Cooperative Research Fellowship Program. Correspondence and requests for materials should be addressed to M.F.R.

Competing financial interests

The authors declare that they have no competing financial interests.